Condon-domain phase diagram and hysteresis size for beryllium

R. B. G. Kramer,[1,2,3] V. S. Egorov,[1,2,4] A. G. M. Jansen,[5] and W. Joss[1,2,6]
[1]*LNCMI, CNRS, BP 166, 38042 Grenoble Cedex 9, France*
[2]*Max-Planck-Institut für Festkörperforschung, Heisenbergstraße 1, 70569 Stuttgart, Germany*
[3]*Institut Néel, CNRS–Université Joseph Fourier, BP 166, 38042 Grenoble Cedex 9, France*
[4]*Russian Research Center "Kurchatov Institute," 123182 Moscow, Russia*
[5]*Service de Physique Statistique, Magnétisme, et Supraconductivité, INAC, CEA-Grenoble, F-38054 Grenoble Cedex 9, France*
[6]*Université Joseph Fourier, BP 53, 38041 Grenoble Cedex 9, France*
(Received 7 May 2010; revised manuscript received 1 July 2010; published 2 August 2010)

The Condon-domain phase diagram for beryllium is determined in magnetic fields up to 10 T and at temperatures down to 1.3 K using a standard ac pick-up coil method to measure the de Haas–van Alphen (dHvA) effect. The detection of the transition point from the homogeneous state to the Condon-domain state (CDS) is based on the extremely nonlinear response to the modulation field resulting from a small irreversibility in the dHvA magnetization. The experimental results are compared with theoretical predictions calculated from the Fermi surface (FS) of beryllium. The width h_m of the hysteresis loop in the CDS is measured in a wide temperature and field region. A model for the hysteresis size is proposed and numerically calculated for the whole phase diagram.

DOI: 10.1103/PhysRevB.82.075101 PACS number(s): 75.45.+j, 71.70.Di, 75.60.−d

I. INTRODUCTION

Condon[1] predicted the formation of diamagnetic domains in nonmagnetic metals, now known as Condon domains. A thermodynamic instability arises according to the Pippard-Shoenberg concept of magnetic interaction[2,3] in the de Haas–van Alphen (dHvA) effect when the amplitude of the oscillatory magnetization signal becomes large enough, i.e., the susceptibility

$$\chi = \mu_0 \frac{\partial M}{\partial B} > 1, \tag{1}$$

where M is the magnetization and B the induction. In this case the stability condition $\mu_0 \partial H/\partial B = 1-\chi > 0$ is not fulfilled for a certain interval of the applied magnetic field H in each dHvA cycle. For an infinitely long rodlike sample (demagnetizing factor $n=0$) the system avoids the instability region by a discontinuous change of the induction B between the two stable states B_1 and B_2 at a certain $H=H_c$. Both stable states have the same free energy (see also Fig. 9) and the interval (B_1, B_2), containing the instability, is forbidden.

For a platelike sample oriented normal to **H** $(n=1)$ the boundary condition $B=\mu_0 H$ is required, so that the induction B cannot change discontinuously and the state with homogeneous magnetization is impossible. The plate breaks up into regions of different magnetization with the inductions B_1 and B_2 within the interval $B_1 < \mu_0 H < B_2$ for $n=1$. The volume fractions of the domains are adjusted in a way that the average induction $\bar{B}=\mu_0 H$ is fulfilled for the whole sample.[1] For a sample with intermediate demagnetizing factor $0<n<1$ the magnetic field interval with domains decreases proportionally to n. Even for samples of arbitrary shape there is without doubt a nonuniform Condon-domain state (CDS) with the same dia- and paramagnetic phases having inductions B_1 and B_2. However, the domain configuration is certainly more complex.

Up to now Condon domains have been observed by different experimental methods; by NMR,[4] μSR spectroscopy[5,6] and they were recently directly observed by Hall probes.[7] All these experiments have in common that two distinct inductions B_1 and B_2 or an induction splitting $\Delta B = B_2 - B_1$ are measured at a given applied field and temperature.

Equation (1) defines the phase boundary between the uniform and the CDS which can be calculated using for example the Lifshitz-Kosevich (LK) formula for the oscillatory dHvA magnetization resulting from the Landau quantization of the conduction electrons in a metal. Theoretical calculations of this boundary exist for several metals.[8,9] However, the above cited measurements yielded only a few points in the (H,T) diagram where Condon domains were actually observed without a complete determination of the Condon-domain phase diagram. An experimental determination of the CDS phase boundary, i.e., where ΔB approaches zero, is difficult and time-consuming.[10] Without doubt, another method for the experimental determination of the phase boundary is needed to obtain sufficient data for a comparison with the theoretical predictions.

Recently, hysteresis was observed in the dHvA effect under the conditions of the CDS.[11] Due to the irreversible magnetization, an extremely nonlinear response to a small modulation field arises in standard ac susceptibility measurements upon entering the Condon-domain state. The out-of-phase part and the third harmonic of the pickup voltage rise steeply at the transition point to the CDS. Moreover, it was shown that the point (H,T) where the hysteresis arises is independent of the sample shape. The threshold character of these quantities allows the measurement of a Condon-domain phase diagram with high precision and in a wide temperature and field range. This offers the possibility for a more detailed comparison with the theoretical calculations.

The CDS boundary of silver has been successfully determined with this method.[12] The FS parameters of the nearly spherical FS of silver are well known. Therefore, for silver the CDS phase diagram in the (H,T) plane can be precisely

predicted using the LK-formula with the Dingle temperature as a parameter.[9] Good agreement was found with experimental data of the dHvA oscillation amplitude in the homogeneous state[13] and for the resulting CDS phase diagram.[12] This demonstrated that the method using the nonlinear response for the determination of the CDS phase boundary is correct.

For beryllium the FS under consideration consists of the well known electron "cigars."[3,14] The curvature of the FS at the extremal cross sections is very small giving rise to a high dHvA amplitude. In addition there are two close dHvA frequencies of 942 and 971 T which lead to a beat in the dHvA amplitude. Due to this frequency beat the CDS phase diagram is more complex compared to silver. Several models have been proposed to calculate a CDS phase diagram for beryllium; a three-dimensional electron gas model using the LK-formula and a purely two-dimensional electron gas model.[8] However, the calculations were in contradiction to experimental data obtained by μSR. This disagreement required new phase-diagram calculations with a modified LK-formula for the intermediate, between two- and three-dimensional, FS of beryllium taking into account the real shape of the electron "cigars."[15] This model is in good agreement with at that time available μSR data. Most recently another theoretical calculation for the phase diagram was proposed using a different model representation of the quasi-two-dimensional Fermi surface of beryllium.[16] However, the very few experimental data available do not allow a complete test of the recent calculations over the whole phase diagram.[6,15]

In this work we determine the experimental Condon-domain phase diagram for beryllium in the whole (H,T) plane for $T>1.3$ K using the appearance of nonlinear response to an ac modulation field for the detection of the phase boundary.[11,12] Moreover, the width of the hysteresis loop in the dHvA effect is measured as function of temperature and magnetic field in the CDS. Finally, a model for the origin of the hysteresis is proposed and numerically derived.

II. EXPERIMENT

A standard pickup coil system was used for the ac measurements of the magnetic susceptibility. The results shown here were measured on the same rodlike sample as in Ref. 11, of sizes $8\times2\times1$ mm^3 with the long side being parallel to [0001]. The magnetic field is applied parallel to the long side of the sample. We found from our measurements a Dingle temperature of $T_D=2.0$ K. The experiments were carried out at temperatures down to $T=1.3$ K in a 10 T superconducting coil with a homogeneity of better than 10^{-5} in a sphere with 1 cm diameter. Some experiments were made in a 16 T coil with a variable temperature insert to measure temperature dependencies at constant magnetic field. The modulation frequency was about 160 Hz.

III. RESULTS

The phase transition point to the CDS can be determined by several methods[12] which are all based on the appearance

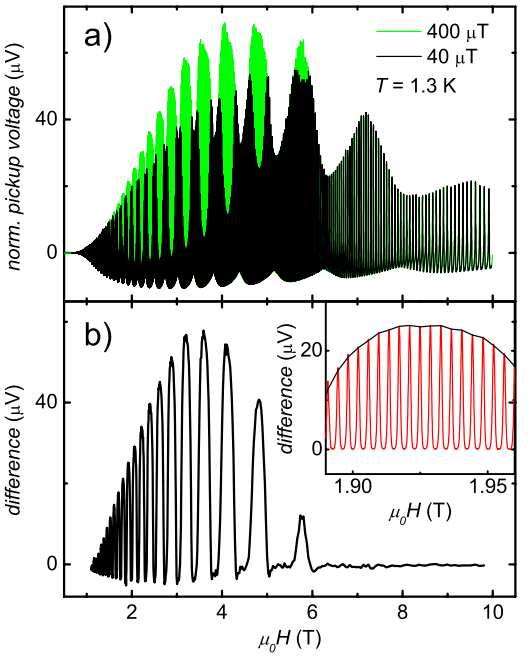

FIG. 1. (Color online) (a) Pickup voltage normalized on the modulation level for high (400 μT) and low (40 μT) modulation level at 1.3 K. Due to hysteresis in the CDS the pickup voltage decreases if the modulation level is of the order or smaller than the hysteresis loop width. (b) Envelope of the difference between both curves of Fig. 1(a) showing the field regions where Condon domains exist for nonzero difference. The inset shows an expanded view of the difference signal with the appearance of hysteresis in a part of each dHvA period.

of hysteresis in the dHvA effect.[11] Figure 1 shows the pickup voltage normalized on the modulation level for low and high modulation amplitude in a large magnetic field range at 1.3 K. Due to the hysteresis in the CDS the response to an ac modulation becomes extremely nonlinear and the first harmonic amplitude of the pickup voltage normalized on the modulation amplitude, usually corresponding to the susceptibility χ, decreases strongly at the paramagnetic part ($\chi>0$) of every dHvA period. The amplitude damping is observed if the modulation level is of the order or smaller than the width of the hysteresis loop. In absence of Condon domains the normalized pickup voltage is independent of modulation level. Therefore, the subtraction of two curves, one measured with high and the other with low modulation level, reveals the magnetic field ranges where Condon domains exist. In other words domains exist if the difference is greater than zero. Figure 1(b) shows the envelope of this function at $T=1.3$ K. The inset presents the detailed difference of both curves in a small region, which corresponds to a cut of the CDS phase diagram at $T=1.3$ K. We see in Fig. 1(b) that there is no difference between the normalized pickup voltages for magnetic fields exceeding 6 T which implies that Condon domains disappear for fields higher than 6 T at 1.3 K.

For the above described method to determine the CDS phase diagram, two field sweeps must be measured for each temperature. In order to detect even very small hysteresis the low modulation level must be as small as possible. There-

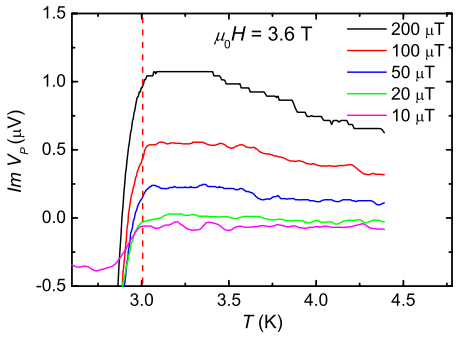

FIG. 2. (Color online) Temperature dependence of the imaginary part of the pickup voltage for several modulation amplitudes at the paramagnetic part of a dHvA oscillation at the beat antinode at 3.6 T. The dashed line indicates the critical temperature T_c =3.0 K where the Condon-domain phase is entered when lowering the temperature.

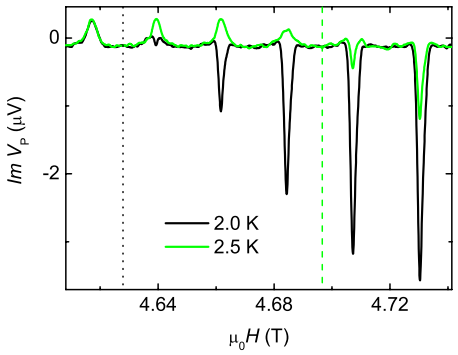

FIG. 3. (Color online) Field dependence of the imaginary part of the pickup voltage measured at 2.0 and 2.5 K with 40 μT modulation amplitude. The steeply increasing negative amplitude is caused by the hysteresis in the CDS. The vertical dotted lines indicate the transition field to the CDS for 2.0 and 2.5 K.

fore, it is difficult to detect by this method the existence of Condon domains at field regions where the hysteresis loop width is small.

It was shown that the out-of-phase part and the third harmonic of the pickup voltage appear with threshold character whenever there is small hysteresis in the dHvA magnetization.[11] A measurement of one of these quantities offers therefore a simple alternative way to determine with high precision the phase boundary of the CDS. Figure 2 shows temperature dependencies of the out-of-phase part of the pickup voltage for a large modulation level range at the beat antinode of the dHvA oscillations at a maximum of χ near 3.6 T. At the critical temperature T_c=3.0 K the out-of-phase signal drops down rapidly upon lowering the temperature. This indicates a sudden phase shift of the ac response with respect to the modulation signal. The phase shift is caused by the emerging hysteresis in the dHvA magnetization.[11] We find the same T_c, indicated by the dashed line in Fig. 2, for all modulation levels showing that the determination of the CDS phase boundary is independent of the used modulation level.

In the following we will use a modulation amplitude of 40 μT. This value is sufficiently small to ensure that the dHvA period is always much bigger than the modulation amplitude h even at low magnetic fields (at $\mu_0 H$=1 T the dHvA period of beryllium is about 1 mT). On the other hand the ac response is still easily detectable. We note that if the modulation amplitude is of the order of the dHvA period the imaginary part and the third harmonic of the pick-up signal show up even in the absence of hysteresis.[3]

Figure 3 shows magnetic field dependencies of the imaginary part of the pickup voltage measured at 2.0 and 2.5 K. The phase of the lock-in amplifier is adjusted such that the signal due to the sample susceptibility is mainly in-phase. dHvA oscillations of small amplitude similar to the waveform in the inset of Fig. 1 are visible in the out-of-phase signal with an amplitude bigger than previously observed in Ref. 11, due to the increased modulation frequency of 160 Hz compared to 21 Hz in Ref. 11. The higher eddy currents explain the appearance of an out-of-phase signal for an homogeneous magnetization. However, Fig. 3 shows threshold character in the arising of negative peaks at magnetic fields where hysteresis occurs indicating the transition to the CDS around the negative peaks in each dHvA period. We see in Fig. 3 that the negative peaks appear at 2.0 K at lower fields than at 2.5 K. At temperatures above 3.0 K all negative peaks disappear and only the small dHvA oscillations due to eddy-current effects remain.

The amplitude of the negative peaks depends on the modulation level, the hysteresis loop width at the particular magnetic field, and on the amplitude of the in-phase part of the pickup voltage, i.e., the susceptibility. Even though the peak amplitude seems to be correlated with the Condon-domain phase diagram being stronger further away from the phase-diagram boundary, we extract from these data only the magnetic field values for which the negative peaks appear for each temperature in order to construct the phase diagram in the next section. The negative peaks arise with threshold character and Fig. 3 shows that the CDS phase boundary can be determined with a precision of about one dHvA period.

It was reported in μSR studies[6,10,15] that Condon domains occur also at the beat nodes of the dHvA oscillations around 2.0 and 2.7 T for 0.5 and 0.8 K, respectively. However, there are only a few temperature dependencies of the induction splitting available from μSR measurements. In other words, the reported temperatures do not represent necessarily the CDS phase boundary for these fields. Figure 4 shows the temperature dependence of the out-of-phase part (a) and the third harmonic (b) of the pickup voltage at the beat node at 2.5 T. A sharp transition at 1.5 K is visible in both traces which indicates that hysteresis arises at this temperature. This means that Condon domains appear indeed at this beat node and the CDS phase boundary is at 1.5 K for 2.5 T.

IV. PHASE DIAGRAM

We have seen that the CDS phase boundary can be determined with high precision using nonlinear response measurements. Due to the hysteresis the out-of-phase signal of the pickup voltage drops sharply. This was measured either at a fixed magnetic field like in Figs. 2 and 4 or at fixed temperature as function of magnetic field like in Fig. 3. All data are

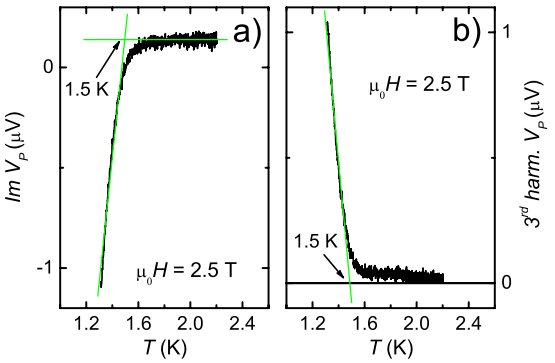

FIG. 4. (Color online) Temperature dependence of the imaginary part (a) and the third harmonic (b) of the pickup voltage measured in the paramagnetic part of a dHvA oscillation at the beat node for 2.5 T with 40 μT modulation amplitude.

compiled to obtain a complete Condon-domain phase diagram in Fig. 5. The solid lines in Fig. 5 are extrapolated guiding lines to the (H,T)-values obtained for the beat antinodes and nodes, respectively. These lines are the envelopes of a substructure consisting of a beating pattern of sharp needlelike domain regions as shown in Fig. 6 where the inset reveals the Condon-domain regions in two successive dHvA periods. For magnetic fields in between these needlelike regions the sample is in the homogeneous state. We see in Fig. 6 that Condon domains appear first for magnetic fields around a beat antinode where the dHvA amplitude is higher. When cooling down the CDS field range extends gradually around the antinodes.

The condition [see Eq. (1)] that a Condon-domain state occurs in a dHvA period is independent of the demagnetization factor. We have found in a test on a platelike sample with the same Dingle temperature that the obtained phase

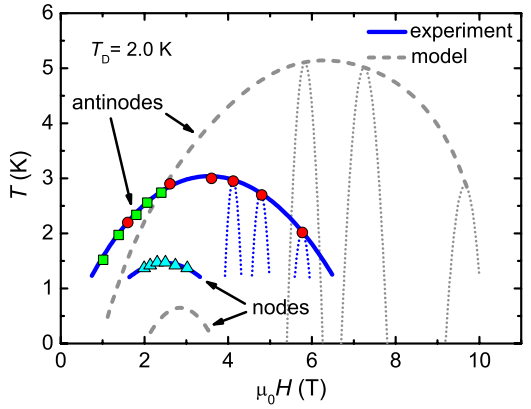

FIG. 5. (Color online) Phase diagram in the (H,T) plane for beryllium. Scatter points indicate the position of the phase boundary at beat nodes and antinodes determined by temperature sweeps (circles and triangles) like in Figs. 2 and 4 and by field sweeps (squares) like in Fig. 3. The solid lines are guiding lines of the phase boundary for beat nodes and antinodes, respectively. The dashed lines show for comparison the recent theoretical model calculation of Refs. 6 and 15. The dotted lines indicate the envelope of the beating substructure of the phase diagram shown in detail in Fig. 6.

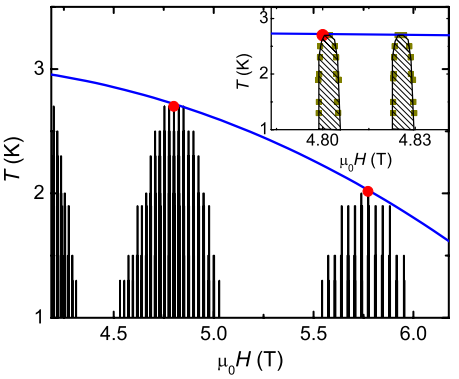

FIG. 6. (Color online) Expanded view of Fig. 5 around the beat maximum at 4.8 T showing the beating substructure of the phase diagram. The slight steps in the envelope of the height of the needlelike stripes results from the limited number of measured temperatures. The expanded view in the inset shows the detailed phase diagram in two successive dHvA periods obtained by field sweeps at constant T. The larger round circles are obtained by T-sweeps at constant H.

diagram is indeed independent of the sample shape. However, this only holds for the envelope of the phase diagram (solid lines in Fig. 5). The substructure depends on the sample shape as the needlelike regions (inset of Fig. 6) are much broader for a platelike sample. The reason for this is that the field range within a dHvA period where domains arise scales with n and is therefore more extended in a platelike sample.[3] In other words, the envelope of the phase diagram in the (H,T)-plane is independent of the demagnetization factor, but not the detailed field region within a single dHvA period.

The phase diagram in Fig. 5 agrees with all reported μSR data.[5,10,15,17] In particular, the observed induction splitting disappeared at the beat antinode near 2.6 T for temperatures higher than 3.0 K. We examined the same beat maximum and found a critical temperature of 2.9 K for our sample.

In Fig. 5 the experimental phase diagram is compared with the calculations made with the modified LK-formula in Refs. 6 and 15. The overall shape of the calculated antinode and node envelope curves is similar to the experimental result. However, there is a clear discrepancy between the predicted temperature and magnetic field ranges of the CDS and the ones we find experimentally. We observe an upper critical field of about 8 T (extrapolation of the guide to the eyes for the antinodes in Fig. 5 to $T=0$) above which domains disappear for all temperatures for our sample with $T_D = 2.0$ K. We see in addition that Condon domains continue to exist at higher temperatures down to lower fields compared to the phase-diagram calculation and that domains exist at the beat nodes up to higher temperatures than predicted. A reason for the discrepancy in the temperature-field values of the phase-diagram boundary can be possibly related to the strong magnetostriction effects in beryllium (see discussion below).

V. HYSTERESIS LOOP SIZE

Another interesting question is the dependence of the hysteresis loop size h_m from temperature and magnetic field. At

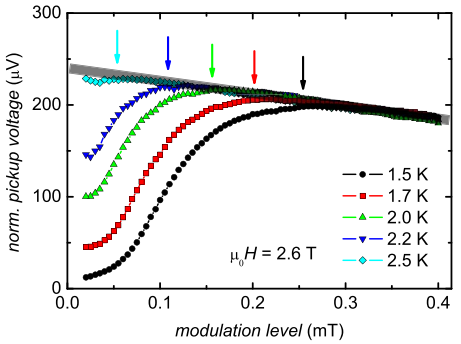

FIG. 7. (Color online) Normalized pickup voltage as function of modulation level for several temperatures in the center of the dHvA oscillation at 2.6 T corresponding to the center of a needlelike stripe like shown in Fig. 6. The arrows indicate the chosen hysteresis sizes h_m.

the CDS phase boundary h_m vanishes. However, the temperature and field dependence of h_m in the CDS might give information about the nature of the irreversible magnetization. We suppose that the hysteresis itself and its size are mainly caused by irreversible domain wall motion or by nucleation of new domain fractions. In the following we will measure the temperature and field dependence within the phase diagram.

As it was shown earlier[11] h_m can hardly be measured directly by Hall probes because of its small magnitude. However, h_m can be indirectly determined by analyzing the response characteristic to an ac modulation field. As shown above, the normalized pickup voltage decreases strongly if the modulation amplitude decreases below the hysteresis size (see Fig. 7). All measurements were made in the center of a dHvA period, i.e., in the center of a needlelike stripe of the phase diagram (see Fig. 6). From Fig. 7 the order of magnitude of h_m can be estimated. However, it is not obvious which modulation level corresponds actually to the real h_m which would be observed with Hall probes. A comparison with direct measurements by Hall probes under the same conditions yields good agreement if we chose for h_m the onset of the decrease in the normalized pick-up voltage indicated by arrows in Fig. 7. All data points obtained in this way are presented in Fig. 8. We see a more or less linear temperature dependence of h_m far enough from the phase boundary. Moreover, h_m is practically independent of H at the lowest measuring temperature far from the phase boundary.

VI. MODEL FOR HYSTERESIS LOOP SIZE

Hysteresis in the CDS is certainly due to irreversible domain wall motion or rearrangement processes of the respective domain volume fractions upon field variation. In the following we analyze the shape and amplitude of the energy barrier in the domain wall between the phases with the inductions B_1 and B_2.

We can write the potential Ω as the sum of the contribution of the magnetoquantum oscillations (taking only the first harmonic of the LK-formula) and the magnetostatic energy

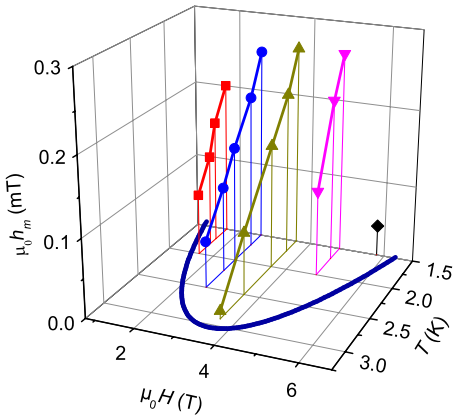

FIG. 8. (Color online) Hysteresis amplitude h_m as function of magnetic field and temperature (data points), determined like in Fig. 7 as a measure for the hysteresis width. The parabola indicates the region of the CDS phase diagram in the (H,T) plane (solid line of the antinodes in Fig. 5).

$$\Omega = a(H,T)\cos\left(2\pi\frac{F}{B}\right) + \frac{1}{2\mu_0}(B-\mu_0 H)^2. \tag{2}$$

with the dHvA frequency F and the oscillation amplitude $a(H,T)$ given by the LK-formula.[3] For inductions B close to the magnetic field H we can develop Eq. (2) setting $B = \mu_0 H + b$

$$\Omega = a(H,T)\cos\left(\frac{2\pi}{p}b\right) + \frac{1}{2\mu_0}b^2 \tag{3}$$

with the dHvA period $p=(\mu_0 H)^2/F$. If the amplitude $a(H,T)$ is big enough, which corresponds to the condition in Eq. (1), then Ω has two minima at b_1 and b_2. Figure 9 shows schematically the potential under this condition.

The states between B_1 and B_2 have extra energy and are not stable. However, in the domain wall the induction B has to cross all values between B_1 and B_2. Therefore, there is an energy barrier (see Fig. 9) separating the states with these inductions whose amplitude ΔE can be calculated. We would

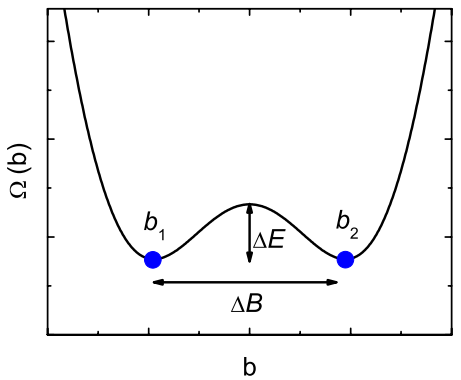

FIG. 9. (Color online) Schematic representation of the Lifshitz-Kosevich potential in the CDS showing two minima corresponding to the domain states with the inductions $B_1=\mu_0 H+b_1$ and $B_2=\mu_0 H+b_2$ and a potential barrier ΔE in the domain wall between the domains.

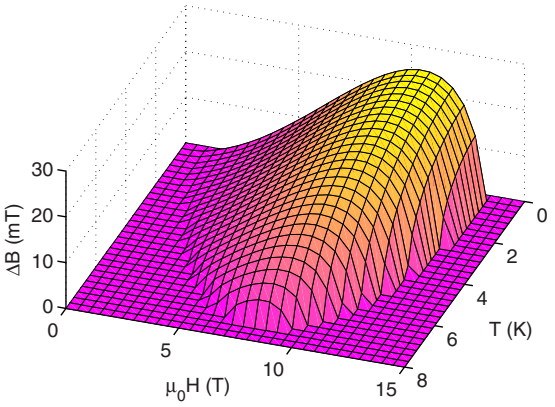

FIG. 10. (Color online) Calculation of the induction difference ΔB between the domains as a function of H and T for a Dingle temperature $T_D=2.0$ K.

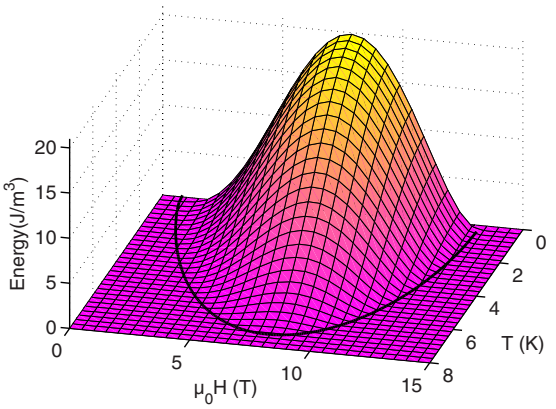

FIG. 11. (Color online) Numerical calculation of the energy barrier ΔE between the domains with the respective inductions B_1 and B_2 as function of H and T for a Dingle temperature $T_D=2.0$ K. The solid line indicates the Condon-domain phase boundary using the cylinder model of Ref. 15.

expect that ΔE scales with the hysteresis width because this energy barrier must be overcome when the domain distribution changes under variation of the applied field.

First, the inductions values B_1 and B_2 of the domains are found by minimization of the free energy

$$\frac{\partial \Omega}{\partial b} = 0, \quad \text{or} \quad a(H,T)\frac{2\pi}{p}\sin\left(\frac{2\pi}{p}b_0\right) = \frac{b_0}{\mu_0}, \tag{4}$$

where

$$b_0 = \frac{b_2 - b_1}{2} = \frac{\Delta B}{2}. \tag{5}$$

The induction difference ΔB between the domains is calculated as a function of H and T in Fig. 10. Here, and in the following calculations we use the "cylinder" model of Ref. 15 which approximates the cigarlike Fermi surface shape of beryllium with a cylinder to determine $\chi(H,T)$ and $a(H,T)$. This idealized model gives a reasonable upper limit for the phase boundary of the domains and should be sufficient to get an idea of the overall behavior of ΔE as a function of H and T.

Once b_1 and b_2 are known we can calculate the amplitude of the energy barrier ΔE using the above formulas

$$\Delta E = \Omega(0) - \Omega(b_1) = a(H,T) - a(H,T)\cos\left(\frac{2\pi}{p}b_1\right) - \frac{b_1^2}{2\mu_0}. \tag{6}$$

A simpler expression for ΔE can be given in good approximation taking into account that the shape of $\Omega(b)$ between b_1 and b_2 is very similar to the cosine function

$$\Omega \approx \frac{\Delta E}{2}\left[\cos\left(\frac{\pi}{b_0}b\right) + 1\right]. \tag{7}$$

Taking the second derivative of this function with respect to b and taking into account that the curvature of Ω is $1/\mu_0(1-\chi)$ at $b=0$, (here χ is positive and $\chi > 1$, we find the following expression:

$$\Delta E = \frac{1}{2\pi^2\mu_0}(\chi - 1)\Delta B^2. \tag{8}$$

This expression for ΔE is similar to the domain wall surface energies calculated earlier.[18,19] Figure 11 shows the numerical calculation of ΔE as a function of temperature and magnetic field.

We see a qualitative agreement between the calculated behavior of ΔE with the observed width of the hysteresis loop in Fig. 8. Both show a maximum at approximately the middle of the magnetic field range of the CDS phase boundary at lowest temperature. There is also good agreement with a recent theoretical calculation where the Rayleigh model was used for the hysteresis.[20] However, we notice that the energy barrier model shows a clear difference from our data near the phase boundary. h_m varies rather steeply when approaching the phase boundary whereas ΔE increases only gradually at the phase boundary. One can say that our model describes well the Condon-domain hysteresis far from the phase boundary where the irreversibility results mainly from domain wall motion. We suggest therefore that close to the phase boundary a mayor contribution to the hysteresis is due to the nucleation of new phase fragments in tubular form. The region where the tubular structure undergoes a transition to a laminar one with stripes could be very narrow compared to the intermediate state of type-I superconductors.[21]

VII. DISCUSSION

We can summarize two main differences in the behavior between beryllium and silver. First, as it was shown recently by using local Hall probes,[7] Condon domains do not emerge to the sample surface in beryllium, appearing only inside the bulk. For silver the measured inductions values of the respective domains are practically the same inside the bulk and on the surface indicating that domains emerge completely to the surface. Second, as it is shown here, the experimental CDS boundary lies inside the closest model and the discrepancy increases for higher magnetic fields in contrast to silver

where at least up to 30 T good agreement was observed with theoretical calculations.[12] We propose that the reason for both findings could lay in the fact that the dHvA effect is always accompanied by magnetostriction oscillations. In the particular case of the CDS this means that domain formation gives rise to different, actually opposite, deformations in the neighboring domains.[22,23]

This deformation varies across the domain walls between neighboring domains and requires extra elastic energy in the domain walls and on the surface. Moreover, the magnetostriction amplitude increases with magnetic field and the amplitude is actually very big especially for beryllium. Beryllium has in comparison to silver a much higher Young modulus and the deformation under the dHvA effect is anisotropic. This idea can qualitatively explain the discrepancy in the phase diagram between theory and experiment at high magnetic fields. Nevertheless, the discrepancy remains for low magnetic fields and for the nodes where the experimentally obtained boundaries are above the calculated ones. It would be of interest to include the influence of magnetostriction on the calculated phase boundaries.

VIII. CONCLUSION

We have measured a complete Condon-domain phase diagram for beryllium at temperatures down to 1.3 K and magnetic fields from 1 up to 10 T. The method based on the detection of the nonlinear response to an ac modulation field provided also information about the substructure of the phase diagram due to the dHvA frequency beat in beryllium. The measurements agree with all data obtained by μSR. Moreover, we have checked that the obtained phase diagram is independent on the sample shape. The method can be easily applied to samples with other Dingle temperatures and other metals.

The hysteresis loop size was measured in a wide region of the CDS phase diagram. In the middle of the phase diagram, far enough from the boundary, the hysteresis loop width increases linearly with decreasing temperature and it is almost constant with magnetic field. Finally, a model for the origin of the hysteresis is proposed. The induction difference between the different domains is numerically derived and the height of the energy barrier separating these two states of induction is calculated. We found that the calculated energy barrier scales well with the observed hysteresis loop width besides in the region close to the phase boundary. We suggest that close to the phase boundary the domain wall motion is not the only reason for the observed hysteresis and that the process of filamentary nucleation of the newly created phase must be taken into account.

ACKNOWLEDGMENTS

We are grateful to N. Logoboy, I. Sheikin, and V. P. Mineev for fruitful discussions.

[1] J. H. Condon, Phys. Rev. **145**, 526 (1966).
[2] A. B. Pippard, Proc. R. Soc. London, Ser. A **272**, 192 (1963).
[3] D. Shoenberg, *Magnetic Oscillations in Metals* (Cambridge University Press, Cambridge, England, 1984).
[4] J. H. Condon and R. E. Walstedt, Phys. Rev. Lett. **21**, 612 (1968).
[5] G. Solt, C. Baines, V. S. Egorov, D. Herlach, E. Krasnoperov, and U. Zimmermann, Phys. Rev. Lett. **76**, 2575 (1996).
[6] G. Solt and V. S. Egorov, Physica B **318**, 231 (2002).
[7] R. B. G. Kramer, V. S. Egorov, V. A. Gasparov, A. G. M. Jansen, and W. Joss, Phys. Rev. Lett. **95**, 267209 (2005).
[8] A. Gordon, M. A. Itskovsky, I. D. Vagner, and P. Wyder, Phys. Rev. Lett. **81**, 2787 (1998).
[9] A. Gordon, I. D. Vagner, and P. Wyder, Adv. Phys. **52**, 385 (2003).
[10] G. Solt, C. Baines, V. S. Egorov, D. Herlach, and U. Zimmermann, Phys. Rev. B **59**, 6834 (1999).
[11] R. B. G. Kramer, V. S. Egorov, A. G. M. Jansen, and W. Joss, Phys. Rev. Lett. **95**, 187204 (2005).
[12] R. B. G. Kramer, V. S. Egorov, V. A. Gasparov, A. G. M. Jansen, and W. Joss, arXiv:1003.4822 (unpublished).
[13] R. B. G. Kramer, V. S. Egorov, A. Gordon, N. Logoboy, W. Joss, and V. A. Gasparov, Physica B **362**, 50 (2005).
[14] J. H. Tripp, P. M. Everett, W. L. Gordon, and R. W. Stark, Phys. Rev. **180**, 669 (1969).
[15] G. Solt, Solid State Commun. **118**, 231 (2001).
[16] N. Logoboy and W. Joss, Solid State Commun. **139**, 191 (2006).
[17] G. Solt, V. S. Egorov, C. Baines, D. Herlach, and U. Zimmermann, Physica B **326**, 536 (2003).
[18] I. A. Privorotskii, JETP Lett. **5**, 230 (1967) [Zh. Eksp. Teor. Fiz. **5**, 280 (1967)].
[19] A. A. Abrikosov, *Fundamentals of the Theory of Metals* (North-Holland, Amsterdam, 1988).
[20] N. Logoboy and W. Joss, Solid State Commun. **140**, 349 (2006).
[21] V. S. Egorov, G. Solt, C. Baines, D. Herlach, and U. Zimmermann, Phys. Rev. B **64**, 024524 (2001).
[22] V. S. Egorov and P. V. Lykov, Sov. Phys. JETP **94**, 162 (2002) [Zh. Eksp. Teor. Fiz. **121**, 191 (2002)].
[23] V. S. Egorov, HAIT J. Sci. Eng. **1**, 647 (2004).